Electronic Supplementary Material (ESI) for Nanoscale Advances.


**Supplementary Information**

# Silica particles with fluorescein-labelled cores for evaluating accessibility through fluorescence quenching by copper

Samuel H. Gallagher, Paul Schlauri, Emanuele Cesari, Julian Durrer and Dominik Brühwiler*

Institute of Chemistry and Biotechnology, Zurich University of Applied Sciences (ZHAW),
CH-8820 Wädenswil, Switzerland
samuel.gallagher@zhaw.ch (SHG), dominik.bruehwiler@zhaw.ch (DB)

Contents

## 1. General synthesis concept

A schematic representation of the core-shell particle formation along with the sample designation is shown in Figure S1.

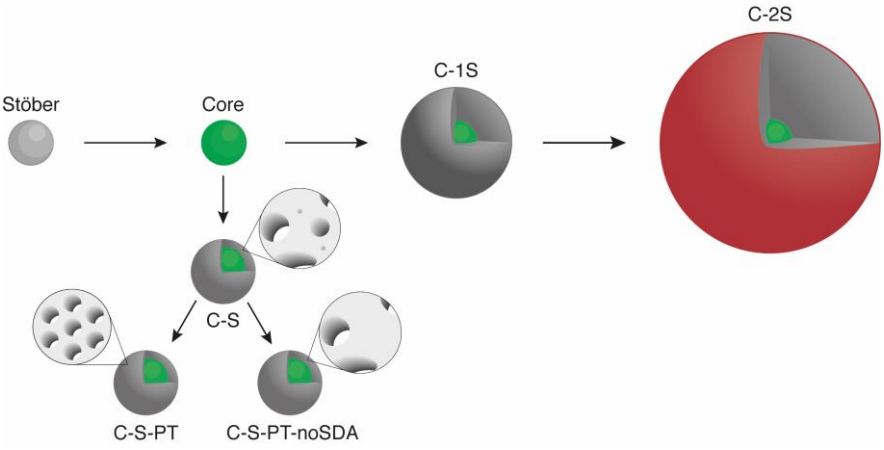


**Figure S1.** Stöber silica particles were synthesised and subsequently labelled with fluorescein. Silica shells were then grown on these fluorescent core particles. Core-shell particles with a double shell (C-2S) were utilised for imaging of the core-shell structure by means of confocal laser scanning microscopy. For this purpose, the external particle surface was labelled with rhodamine. For the accessibility studies (quenching with $Cu^{2+}$), particles with a thin shell were used (C-S). These particles were pseudomorphically transformed to introduce defined mesopores (C-S-PT). The control sample C-S-PT-noSDA was obtained by conducting a transformation in the absence of the structure-directing agent.

## 2. Shell growth

Figure S2 shows SEM images of samples taken at different times during the shell growth of the C-1S particles. Note the small secondary particles.

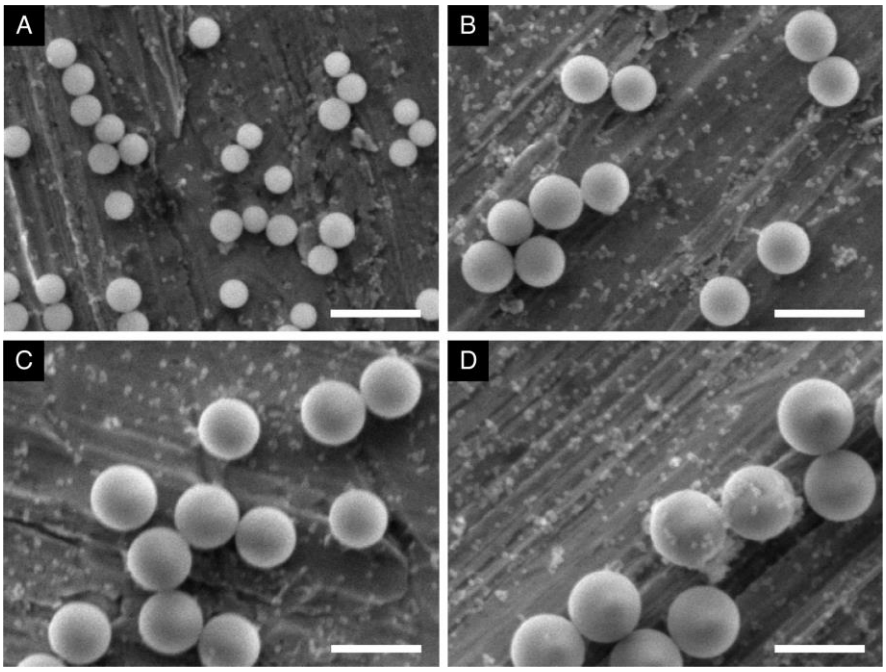


**Figure S2.** SEM images presenting the shell growth for C-1S particles at different time points: 20 min (A), 50 min (B), 80 min (C) and 110 min (D). The large particles are stable primary particles and the small dots on the surface of the copper tape and on the primary particles are unstable secondary particles. The scale bars are 1 µm.

The particle size can be predicted with eq. S1, assuming that particle growth occurs exclusively by monomer addition.[1] The particle population should therefore not increase with time. The theoretical and the experimental values show good correlation (Figure S3), although the theoretical model of monomer addition overestimates the particle size at the early stages of the growth process due to the formation and consumption of unstable secondary particles.

$$d = d_{\mathrm{core}} \cdot \sqrt[3]{\frac{m_{\mathrm{core}} + (V_{\mathrm{TEOS}} \cdot \rho_{\mathrm{TEOS}} \cdot 0.2884)}{m_{\mathrm{core}}}} \qquad \text{(S1)}$$

The diameter and the mass of the core particles is $d_{\mathrm{core}}$ and $m_{\mathrm{core}}$, respectively. $V_{\mathrm{TEOS}}$ is the volume of added TEOS (addition rate multiplied with reaction time) and $\rho_{\mathrm{TEOS}}$ is the density of TEOS. The factor 0.2884 takes into account the $SiO_2$ content of TEOS.

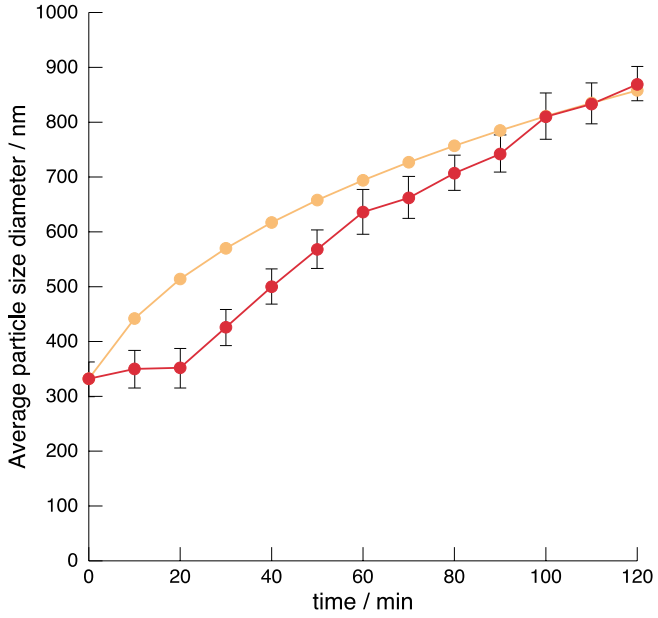


**Figure S3.** Theoretical (●) and experimental (●) particle diameters at different times during the shell growth. The average of 100 particles (over five SEM images from five different spots) was taken for the determination of the experimental average particle size. The theoretical values were calculated according to eq. S1. The core particles used for this experiment had an average diameter of 330 nm.

### 3. Pseudomorphic transformation

Figure S4 shows SEM images of C-S particles before and after pseudomorphic transformation (PT). The structure-directing agent (SDA) was extracted by cation exchange according to a previously published procedure.[2] The spherical morphology and the particle size have been retained. A narrow pore size distribution centred at 4.1 nm was obtained after PT (Figure S5).

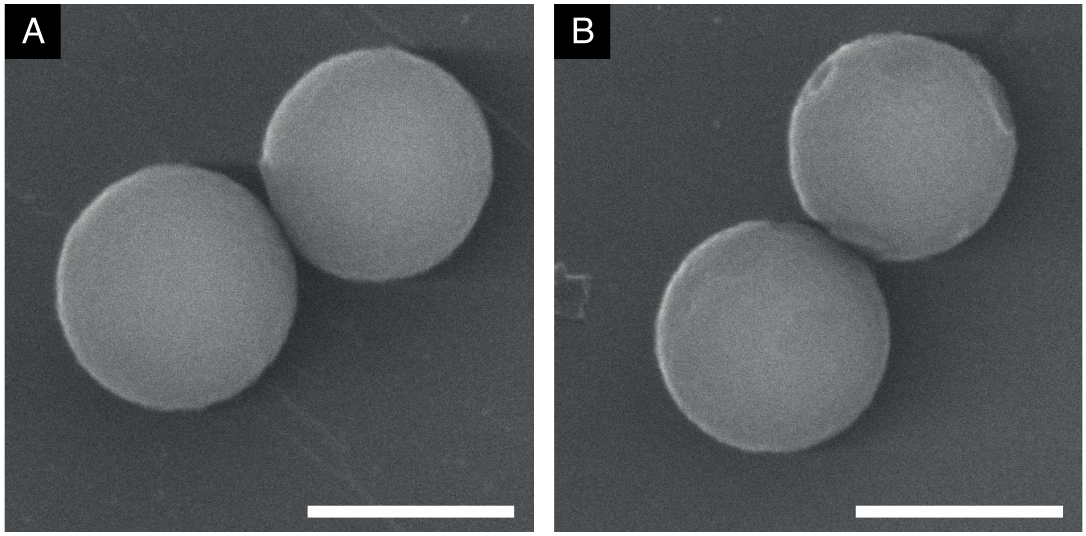


**Figure S4.** SEM images of C-S particles before (A) and after PT in the presence of cetyltrimethylammonium bromide as a structure-directing agent (B). The scale bars are 500 nm.

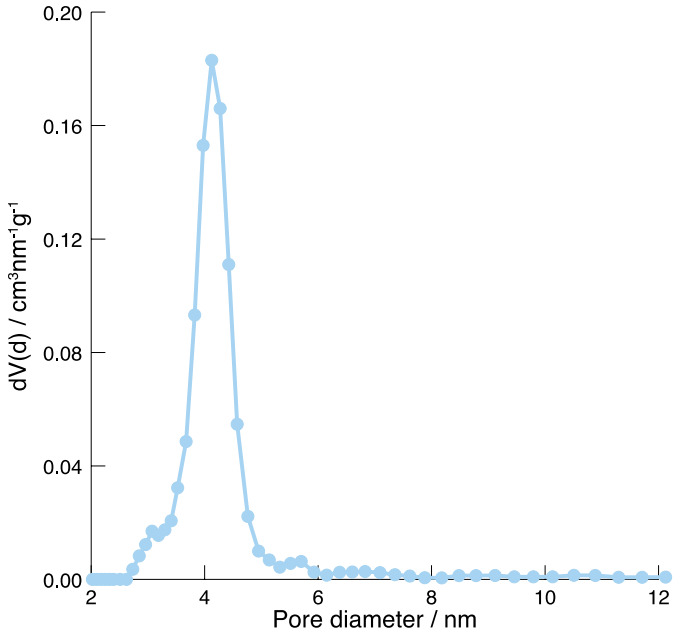


**Figure S5.** Pore size distribution of C-S particles after PT and extraction of the SDA.

## 4. Pore volume data

Pore volume data of the samples are summarised in Table S1.

**Table S1.** Gas sorption data taken from argon adsorption isotherms of core particles, as-synthesised core-shell (C-S), calcined core-shell (C-S-cal), pseudomorphically transformed and calcined core-shell (C-S-PT-cal), pseudomorphically transformed and extracted core-shell (C-S-PT-ext), C-S particles after transformation without SDA (C-S-PT-noSDA), C-S particles after transformation without NaOH (C-S-PT-noNaOH), C-S particles after transformation without ageing (C-S-PT-noAgeing). $V_{\mu}$ is the volume contribution of all pores smaller than 2 nm (micropore volume), $V_{meso}$ is the volume contribution of pores with sizes between 2 and 7 nm, $V_{tot}$ is the total pore volume up to 40 nm.

| Sample | $V_{\mu}$ (< 2 nm) [$cm^3g^{-1}$] | $V_{meso}$ (2 – 7 nm) [$cm^3g^{-1}$] | $V_{tot}$ [$cm^3g^{-1}$] | Average pore diameter [nm] |
|---|---|---|---|---|
| Core | - | - | 0.02 | - |
| C-S | 0.13 | 0.06 | 0.19 | - |
| C-S-cal | 0.05 | 0.03 | 0.08 | - |
| C-S-PT-cal | 0.00 | 0.15 | 0.17 | 4.1 |
| C-S-PT-ext | 0.00 | 0.12 | 0.14 | 4.2 |
| C-S-PT-noSDA | 0.01 | 0.02 | 0.03 | - |
| C-S-PT-noNaOH | 0.01 | 0.07 | 0.10 | - |
| C-S-PT-noAgeing | 0.03 | 0.06 | 0.10 | - |

## 5. Reversibility of quenching with copper

$Cu^{2+}$ quenches the fluorescence of the fluorescein-labelled core-shell particles. The fluorescence is restored upon addition of an excess of $Ca^{2+}$ (Figure S6).

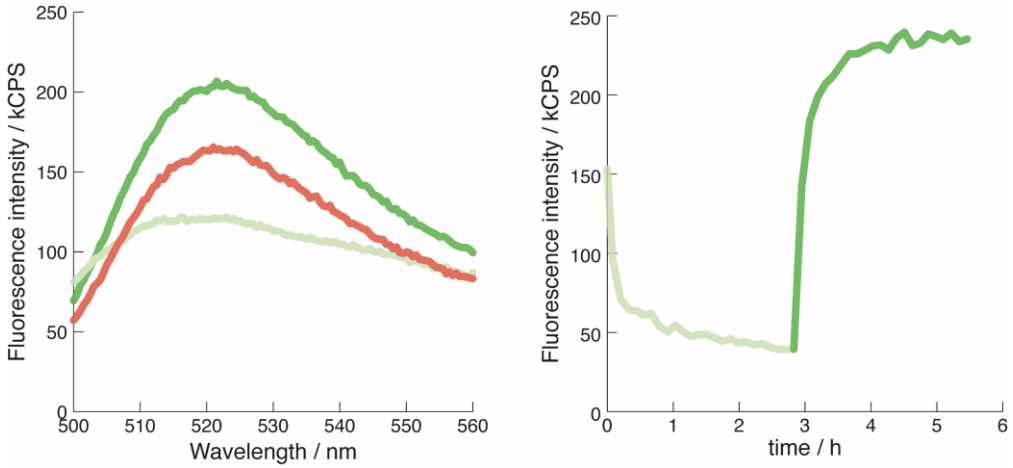


**Figure S6.** Left: Fluorescence spectra of C-S particles (●), after quenching with $Cu^{2+}$ (●) and after the addition of $Ca^{2+}$ (●). Right: Time-dependent measurement of the fluorescence intensity of C-S particles (at 519 nm) with the addition of an excess of 24 eq. of $Cu^{2+}$ (relative to the amount of FITC used for the labelling) at 0 h followed by the addition of an excess of 24 eq. of $Ca^{2+}$ at 3 h.

## 6. Accessibility of co-condensed fluorescein-labelled MCM-41

As-synthesised MCM-41 particles co-condensed with APTES/FITC were used to evaluate the accessibility of fluorescein located in mesopores, which are filled with SDA. As shown in Figure S7, the fluorescence of these particles can be efficiently quenched. It can be concluded from this result that a pore diameter of 4 nm does not hinder the diffusion of $Cu^{2+}$ even if the pores are filled with SDA.

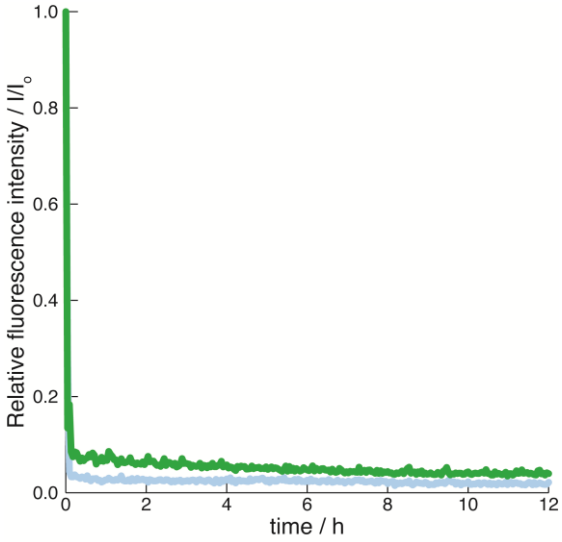


**Figure S7.** Relative fluorescence intensities as a function of time for core particles (•) and as-synthesised MCM-41 particles co-condensed with APTES/FITC (•) following the addition of $Cu^{2+}$ at 0 h.

## 7. Reproducibility of time-dependent fluorescence measurements

Repetitions of the time-dependent quenching experiments were completed. Figure S8 shows three independent measurements for C-S and C-S-PT particles.

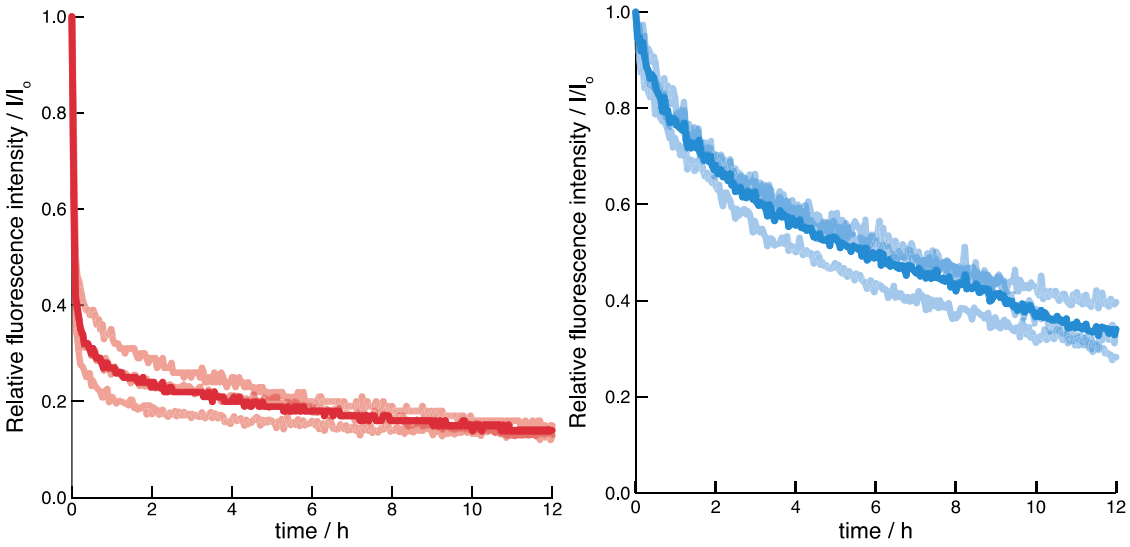


**Figure S8.** Left: Relative fluorescence intensities of C-S particles as a function of time after the addition of $Cu^{2+}$ at 0 h. The average (•) and three independent measurements (•) are shown. Right: Relative fluorescence intensities of C-S-PT particles as a function of time after the addition of $Cu^{2+}$ at 0 h. The average (•) and three independent measurements (•) are shown.

## 8. References

1 S.-L. Chen, P. Dong and G.-H. Yang, The Size Dependence of Growth Rate of Monodisperse Silica Particles from Tetraalkoxysilane, *J. Colloid Interface Sci.*, 1997, **189**, 268–272.

2 N. Lang and A. Tuel, A Fast and Efficient Ion-Exchange Procedure To Remove Surfactant Molecules from MCM-41 Materials, *Chem. Mater.*, 2004, **16**, 1961–1966.